Phase-sensitive detection of signals with non-sinusoidal modulation: The rectangular wave modulation case and its application to the photoacoustic technique

J. B. Rojas-Trigos[1], F. D. Brindis-López[1,2], and A. Calderón[1]
[1]*Centro de Investigación en Ciencia Aplicada y Tecnología Avanzada, del Instituto Politécnico Nacional. Av. Legaria # 694, Col. Irrigación, C.P. 11500, México D. F.*
[2]*Unidad Interdisciplinaria en Ingeniería y Tecnologías Avanzadas, del Instituto Politécnico Nacional. Av. IPN # 2580, Barrio La Laguna Ticomán, C.P. 07340, México D. F.*

E-mail: jrojast@ipn.mx

(Received 2 May 2013, accepted 19 August 2013)

Abstract

The phase-sensitive detection is a powerful mathematical tool in the recovering of signals, at low noise/signal ratio, in many areas of science and engineering. Specifically in Photothermal Science and Techniques (in all its variants) is essential the implementation of a stage of amplification and filtering (for example, by means of a lock-in amplifier) of the obtained photothermal signal from a measurement system, before to analyze the experimental data. Due to the general preference of sinusoidal modulation in the modelling of the generation of the photothermal signal, it is a common practice to neglect the information contained in superior harmonics, since sinusoidal functions are used as reference signals in the phase-sensitive detection stage. However, because the modulation of the optical excitation is often produced by means of a mechanical modulator (or directly by electronic control of a shutter integrated in the laser source, using a TTL signal) the photothermal signal is in fact modulated by a rectangular wave train, and therefore the neglected harmonics could be relevant, depending on the thermal regime in which the measurement is performed, and the thermal relaxation processes involved. In this paper, the phase-sensitive detection is applied to a square-integrable signal with non-sinusoidal modulation, analyzing the influence of the harmonics in the amplified output signal in frequency domain, and it is demonstrate that considering reference functions congruent to the modulations of the photothermal signal, the contribution of the superior harmonics do not vanishes.

Keywords: Fourier analysis, orthogonal functions, Phase-sensitive detection, Photoacoustic technique, Photothermal techniques, Thermal properties.

Resumen

La detección sensible en fase es una herramienta matemática poderosa en la recuperación de señales, a baja razón ruido/señal., en muchas áreas de la ciencia e ingeniería. Específicamente en las ciencias y técnicas Fototérmicas (y en sus variantes existentes), es esencial la implementación de una etapa de amplificación y filtrado (por ejemplo, mediante el uso de un amplificador lock-in) de las señales fototérmicas obtenidas mediante los sistemas de medición, antes de analizar los datos experimentales. Debido a la preferencia generalizada de utilizar una modulación sinusoidal al modelar la generación de la señal Fototérmica, es práctica común el despreciar la información contenida en los armónicos superiores, puesto que en la etapa de detección sensible en fase son usadas señales de referencia sinusoidales. Sin embargo, ya que la modulación de la excitación óptica es frecuentemente producida mediante el uso de moduladores mecánicos (o directamente mediante el control electrónico del obturador de la fuente laser usando una señal TTL), la señal Fototérmica está de hecho modulada mediante un tren periódico de ondas rectangular, y por tanto, los armónicos usualmente despreciados pueden ser de relevancia, dependiendo del régimen térmico dentro del cual se realiza la medición y de los procesos de relajación térmica involucrados. En este trabajo, la detección sensible en fase es aplicada a una señal cuadráticamente integrable, con una modulación no sinusoidal, analizando la influencia de los armónicos en la señal de salida amplificada, en el dominio de la frecuencia y demostrándose que al considerar funciones de referencia congruentes con la modulación de la señal fototérmicas, la contribución de los armónicos superiores no es nula.

Palabras Clave: Análisis de Fourier, Detección sensible en fase, Funciones ortogonales, Propiedades térmicas, Técnica Fotoacústica, Técnicas Fototérmicas.

PACS: 02.30.Nw, 02.30.Jr, 43.58.Kr, 44.05.+e, 44.10.+i, 65.20.+w, 65.40.-b, 60.90.+v **ISSN 1870-9095**

I. INTRODUCTION

The Lock-in amplifier, based on the principle of the Phase-Sensitive Detection (PSD), is an extraordinary tool for signal's recovery, indispensable in many of the measurements systems in today physics. In a general description, the Lock-in amplifier [1, 2, 3] allows to remove, from an electrical input signal, the components which are outside of a very narrow frequency window centred on a reference frequency; which reduces significantly the contamination of the signal by the ambient noise. The almost free-noise signal is then easily amplified, maintaining a very high signal/noise ratio (SNR). This process of filtering and amplification is composed by four basic stages: a) The AC amplification stage; b) The Phase-sensitive detection (PSD) stage; c) The Low-pas filtering (LPF) stage and; d) The DC amplification stage. The Lock-in amplifier block diagram is shown in Figure 1.

In the AC amplification stage, the input signal (scrambled with the ambient noise) is amplified and filtered, usually by variable band-pass filters. In this first stage, much of the noise is removed from the total signal. From a reference signal, the Lock-in amplifier constructs a time-dependent reference function e_r^{IP}, using the internal oscillator or the reference signal itself (this block is referenced as the in-phase reference generator), and a second reference function e_r^{Q} by a phase shifting. Every reference function is then multiplied by the signal $f(t) + n(t)$ (out coming from the AC amplification), to generate the pair of functions $f_i^k(t) + n_i^k(t) = [f(t) + n(t)]\, e_r^k$, with $k = IP, Q$. This is the PSD stage, the main feature of the Lock-in amplifier.

Next, in the LPF stage, the functions $f_i^k(t) + n_i^k(t)$ are filtered by a low-pass filter with transfer function $H(\omega)$, removing all the frequencies above from a cut-off frequency ω_c. The output signals are then almost noise-free, since the LPF is essentially an exponential integrator and the noise is mostly random.

And finally, the signals are passed through a DC amplifier.

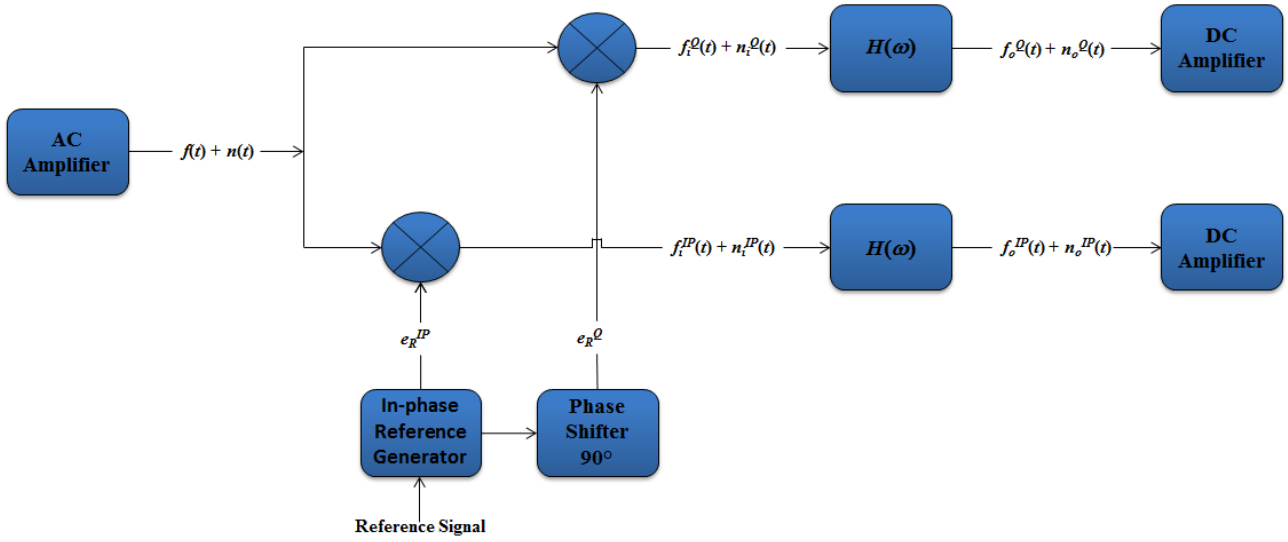

FIGURA 1. Block diagram of the functioning of the Lock-in amplifier. Here, X represents the multiplication blocks.

In this paper we consider that the reference functions e_r^{IP} and e_r^{Q} are two rectangular waves (the periodic versions of the boxcar function [4]) having the next Fourier expansions:

$$e_r^k(t) = \sum_{m=-\infty}^{\infty} d_m^k \cdot e^{i\omega_m t}, \qquad (1)$$

$$d_m^k = \frac{\mathrm{Sinc}(m/2)}{2} \cdot \left[\delta_{k,IP} + e^{-im\pi}\delta_{k,Q}\right].$$

Where, $\omega_m = m\omega$, being ω the angular modulation frequency of the reference ($\omega = 2\pi f^{-1}$), and Sinc is the cardinal Sine function [4]. Also consider that the input function $f_i(t)$ is a square-integrable (not necessarily periodic) function, having a Fourier expansion in terms of harmonics of ω, as Eq. (2) shown:

$$f_i(t) = \sum_{m=-\infty}^{\infty} R_m(\omega) \cdot e^{i\omega_m t}. \qquad (2)$$

In Figure 2, the reference functions (signals) e_r^{IP} and e_r^{Q} are shown for $\omega = \pi\, s^{-1}$, calculated for the first 21 harmonics, during a time interval of 1 s. The observed oscillations near to the discontinuity points of the boxcar function (at $t = 0.5$ s for this example) are consequence of the well-known Gibb's phenomenon. However, the functions expressed in Eq. (1) are differentiable, converging at the discontinuity points to the average values [4, 5]. In fact, both Eq. (1) and Eq. (2) are

analytical, square-integrable functions in the entire time and frequency domains.

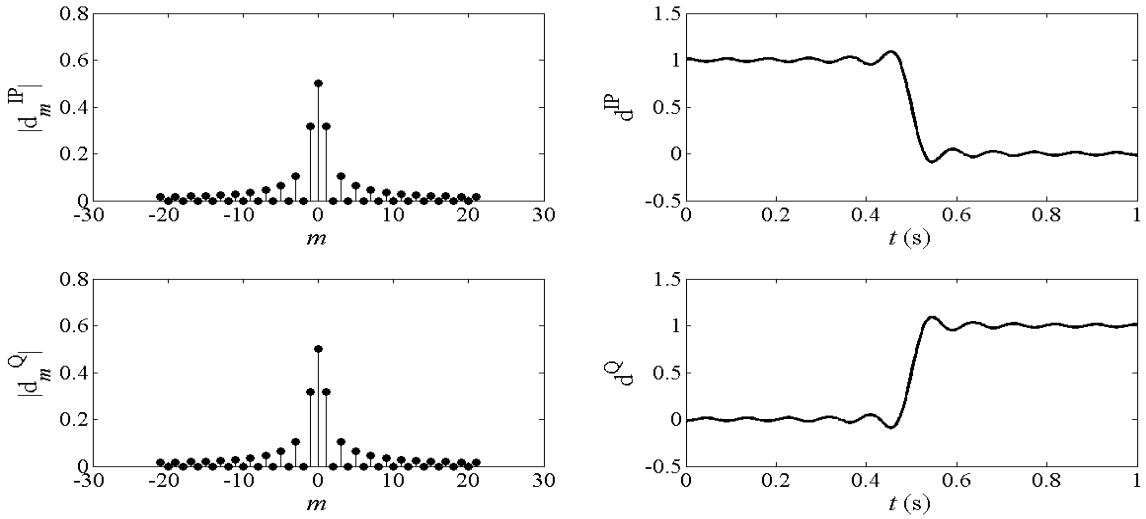

FIGURA 2. Rectangular wave reference functions, and their Fourier coefficients (m_{max} = 21), for $\omega = \pi\,\mathrm{s}^{-1}$.

II. CALCULUS FOR THE PSD AND LPF STAGES

Due to many of the Photothermal (PT) techniques are resolved in frequency domain, we focus our attention to the PSD (and mostly of our calculations) in frequency domain. From Eqs. (1, 2), and by means of the unitary Fourier Transform [5], the input signals $\hat{f}_i^k$ are given as follows:

$$\hat{f}_i^{\,k}(\omega') = \sqrt{2\pi}\sum_{m=-\infty}^{\infty} D_m^k(\omega')\cdot\delta(\omega'-\omega_m),$$
$$D_m^k(\omega') = \sum_{j=-\infty}^{\infty} d_{m-j}^k R_j(\omega'). \tag{3}$$

It is well known that the transfer function of the RC first order LPF is given by:

$$H(\omega') = \frac{1}{\sqrt{2\pi}}\frac{\omega_c}{\omega_c + \mathrm{i}\omega'}. \tag{4}$$

In Eq. (4), $\omega_c = (RC)^{-1}$ is the cut-off frequency of the LPF defined by the product of the electrical resistance and capacitance values of the LPF [4]. Using the Convolution Theorem, the output signals from the LPF are calculated to be:

$$\hat{f}_o^{\,k}(\omega') = \sqrt{2\pi}\omega_c\sum_{m=-\infty}^{\infty}\frac{D_m^k\cdot\delta(\omega'-\omega_m)}{\omega_c+\mathrm{i}\omega_m}\ . \tag{5}$$

And therefore, related to the next Fourier expansion:

$$f_o^k(t) = \sum_{m=-\infty}^{\infty} F_m^k(\omega_c,\omega)\cdot \mathrm{e}^{\mathrm{i}\omega_m t}, \tag{6}$$

where

$$F_m^k(\omega_c,\omega_0) = \sum_{j=-\infty}^{\infty}\frac{d_{m-j}^k\cdot R_j(\omega)}{1+\mathrm{i}\left(\dfrac{m\omega}{\omega_c}\right)}\ .$$

To end this section, we would like to establish some useful results for the next section. Be the truncation x_T for a given signal $x(t)$, defined as follows,

$$x_T \equiv \begin{cases} x(t) & |t| \le T/2, \\ 0 & \text{elswhere.} \end{cases} \tag{7}$$

Where the function $x(t)$ had an expansion in the Fourier basis. From the definition of average power P, we have,

$$P = \lim_{T\to\infty}\left[\frac{1}{T}\int_{-T/2}^{T/2}|x(t)|^2\,\mathrm{d}t\right] = \int_{-\infty}^{\infty}\left[\lim_{T\to\infty}\frac{|\hat{x}_T(\omega')|^2}{T}\right]\mathrm{d}\omega'\ . \tag{8}$$

The quantity in brackets in Eq. (8) is called the spectral power density S, *i.e.*

$$S(\omega') \equiv \lim_{T\to\infty}\frac{|\hat{x}_T(\omega')|^2}{T}. \tag{9}$$

In the next section, we calculate the spectral power densities S_i^k and S_o^k, and demonstrate how the superior harmonics are relevant in the amplifications of a signal with a rectangular wave modulation.

III. CALCULATION OF THE AVERAGE POWER

Because of the f_{i}^{k} and f_{o}^{k} signals have an expansion in the Fourier basis, their truncate versions also have an expansion in Fourier basis, and therefore, we can calculate their Fourier transforms,

$$\hat{f}_{\mathrm{i}}^{k} = \mathrm{T}\sum_{m=-\infty}^{\infty} D_m^k \cdot \mathrm{Sa}\left((\omega' - \omega_m)\mathrm{T}/2\right),$$
$$\hat{f}_{\mathrm{o}}^{k} = \mathrm{T}\sum_{m=-\infty}^{\infty} F_m^k \cdot \mathrm{Sa}\left((\omega' - \omega_m)\mathrm{T}/2\right). \tag{10}$$

In Eq. (10), Sa is the modulation function, closely related with the Sinc function. So, from Eqs. (9) and (10), the spectral power densities are written as follows,

$$S_{\mathrm{i}}^{k} = 2\pi\sum_{m=-\infty}^{\infty} \left|D_m^k\right|^2 \cdot \delta(\omega' - \omega_m),$$
$$S_{\mathrm{o}}^{k} = 2\pi\sum_{m=-\infty}^{\infty} \left|F_m^k\right|^2 \cdot \delta(\omega' - \omega_m). \tag{11}$$

In Eq. (11) we use the relation between the Dirac Delta and the Sa function,

$$\delta(\omega' - \omega_m) = \lim_{\mathrm{T}\to\infty} \frac{\mathrm{T}}{2\pi} \cdot \mathrm{Sa}^2\left((\omega' - \omega_m)\mathrm{T}/2\right). \tag{12}$$

Similar expressions where reported by Mandelis for sinusoidal reference functions for analog LIA [3]. He demonstrates that the relevance of superior harmonics in the total average power is, in fact, negligible. However, the calculations of Mandelis were based in the assumption that the PA signal had sinusoidal modulation, which is inconsistent with an experimental setup where the modulation of the light source is done by using a mechanical modulator (chopper), or by a TTL signal controlling the laser shutter.

IV. PHOTOACOUSTIC SIGNAL FOR SQUARE WAVE MODULATION

Consider an arrangement of three homogenous medium, labelled here by j = (b), (s), (g), with cylindrical symmetries, as shown in Figure 3.

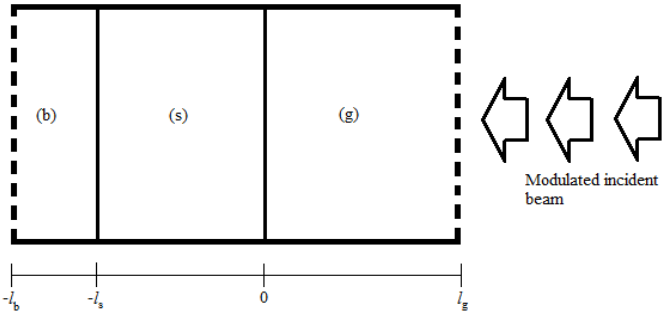

FIGURA 3. Representative scheme of the system studied and the spatial configuration of the different possible medium.

Such medium system will be optically excited by a coherent monochromatic beam, modulated in amplitude by a rectangular wave train, $\mathrm{T}_{\mathrm{mod}}(t)$, expressed in Eq. (13) in the exponential Fourier basis:

$$\mathrm{T}_{\mathrm{mod}}(t) = \sum_m \frac{\mathrm{Sinc}(m/2)}{2} \mathrm{e}^{\mathrm{i}\omega_m t}. \tag{13}$$

If the medium (g) is not absorbing in the wavelength of the beam, and the energy of it is absorbed and transformed into heat by non-radiative processes by medium (s), the heat will diffuses along the system. By means of the parabolic heat diffusion equation [6], and proposing that the variations of the temperature distributions Θ_j (measured respect the ambient temperature T_{amb}) are given by,

$$\Theta_j(t,z) = \sum_m R_{jm}(\omega,z)\mathrm{e}^{\mathrm{i}\omega_m t}. \tag{14}$$

The coefficients R_{jm} are given by the solutions of next ordinary differential equation system:

$$\frac{\mathrm{d}^2}{\mathrm{dz}^2} R_{jm} - \sigma_{jm}^2 R_{jm} = -g_{jm}. \tag{15}$$

In Eq. (15), α_j, $\sigma_{jm}(\omega) = (\mathrm{i}m\omega\alpha_j^{-1})^{1/2}$ are the thermal diffusivity and the complex diffusion coefficient for medium j, respectively, and the functions g_{jm} are the expansion coefficients in the Fourier basis of the heat source,

$$G_j(t,z) = \sum_m g_{jm}(z)\mathrm{e}^{\mathrm{i}\omega_m t},$$
$$g_{jm}(z) = \frac{g_{sm}(z)\cdot\mathrm{Sinc}(m/2)}{2\kappa_{\mathrm{s}}} \cdot \delta_{j,\mathrm{s}}. \tag{16}$$

Where κ_{s} is the thermal conductivity of the sample, and $g_{sm}(z)$ depends on the thermal relaxation mechanisms under consideration. The solution of Eq. (15) is constrained by continuity conditions of temperature distribution and heat flux at the interfaces $z = -l_{\mathrm{s}}$ and $z = 0$, *i.e.*

$$R_{gm}(\omega,0)=R_{sm}(\omega,0),$$

$$R_{bm}(\omega,-l_s)=R_{sm}(\omega,-l_s),$$

$$\kappa_g\frac{d}{dz}R_{gm}(\omega,z)\Big|_{z=0}=\kappa_s\frac{d}{dz}R_{sm}(\omega,z)\Big|_{z=0}, \quad (17)$$

$$\kappa_b\frac{d}{dz}R_{bm}(\omega,z)\Big|_{z=-l_s}=\kappa_s\frac{d}{dz}R_{sm}(\omega,z)\Big|_{z=-l_s}.$$

Solving the Eq. (15) under the specified boundary conditions, the temperature variations Θ_g and Θ_b are given by the following expressions,

$$\Theta_g=\sum_{m\neq 0}R_{sm}(\omega,0)e^{(i\omega_m t-\sigma_{gm}z)},$$

$$\Theta_b=\sum_{m\neq 0}R_{sm}(\omega,-l_s)e^{(i\omega_m t+\sigma_{bm}(z+l_s))}. \quad (18)$$

Where,

$$R_{sm}(\omega,0)=\int_{-l_s}^{0}g_{sm}(z')\cdot K_{>}(0,z',\omega)dz,$$

$$R_{sm}(\omega,-l_s)=\int_{-l_s}^{0}g_{sm}(z')\cdot K_{<}(-l_s,z',\omega)dz. \quad (19)$$

And,

$$K_{>}=\frac{\mathrm{Cosh}(\sigma_{sm}(z'+l_s)+\eta_{bs}\mathrm{Sinh}(\sigma_{sm}(z'+l_s))}{\sigma_{sm}[\mathrm{Sinh}(\sigma_{sm}l_s)+\eta_{bs}\mathrm{Cosh}(-\sigma_{sm}l_s)]},$$

$$K_{<}=\frac{\mathrm{Cosh}(\sigma_{sm}z')}{\sigma_{sm}[\mathrm{Sinh}(\sigma_{sm}l_s)+\eta_{bs}\mathrm{Cosh}(-\sigma_{sm}l_s)]}. \quad (20)$$

Where $K_{<,>}$ are the Green's functions associate with (15), and the coefficient $\eta_{bs} = \varepsilon_b\varepsilon_s^{-1}$ is the quotient of the thermal effusivities ε_j of the respective medium [7, 8, 9]. The combination of Eqs. (18-20) give us the temperature variations in the mediums (b) and (g). All these expressions are suitable to apply in others PT techniques, such as Photopyroelectric detection and Infrared Photothermal Radiometry detection [11, 12, 13, 14].

V. PHOTOACOUSTIC DETECTION

If the Beer-Lambert Absorption Law is taken into account, and if the heat transport is mainly due to phonon contribution, the function g_{sm} is written as follows:

$$g_{sm}(z)=(1-R)I_0\beta\cdot e^{\beta z}. \quad (21)$$

Where R, β, are the reflection coefficient and the optical absorption coefficient (at the current wavelength), respectively; and I_0 is the power density of the incident beam.

A. Open PA cell configuration

To put it briefly, for this PA configuration the backing medium (b) is the air enclosed in the acoustic chamber (Figure 4a).

Thus, the generated heat will diffuse trough the sample produces modulated adiabatic expansions of a thin boundary layer of the gas in the acoustic chamber that generates acoustic pressure oscillations ΔP_b. In analogy to the Thermal Piston model, developed by Rosencwaig and Gersho [11], the acoustic pressure oscillations are given by:

$$\Delta P_b=\frac{\gamma P_{atm}}{l_b T_{amb}}\sum_{m\neq 0}R_{sm}(\omega,-l_s)\int_{-l_s-2\pi\mu_{bm}}^{-l_s}e^{\sigma_{bm}(z+l_s)}dz. \quad (22)$$

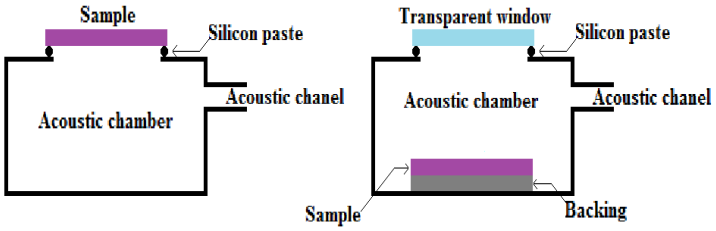

FIGURA 4. Schematics of: (a) An open photoacoustic cell, and (b) a closed photoacoustic cell.

In Eq. (22), P_{atm} is the atmospheric pressure; l_b,γ, $\mu_{bm} = (2\alpha_b/\omega_m)^{1/2}$ are the thickness, the adiabatic coefficient and the thermal diffusion length (corresponding to harmonic m) of the enclosed air in the acoustic chamber, respectively. Using the equations (18-22), and considering that the thermal effusivity of a solid is much greater than the thermal effusivity of a gas (therefore, the coefficient $\eta_{bs} \sim 0$), the acoustic pressure takes the form expressed in Eq. (23)

$$\Delta P_b=P_{b0}\sum_{m\neq 0}\frac{\mathrm{Sinc}(m/2)}{m\omega\mathrm{Sinh}\sigma_{sm}l_s}T_m^{T},$$

$$T_m^{T}=r_{sm}\left[\frac{e^{-\beta l_s}(r_{sm}\mathrm{Cosh}\sigma_{sm}l_s+\mathrm{Sinh}\sigma_{sm}l_s)-r_{sm}}{1-r_{sm}^2}\right]. \quad (23)$$

Where P_{b0} is an amplitude factor independent of the modulation frequency, and $r_{sm} = \beta\sigma_{sm}^{-1}$. If occurs that $\mu_{sm} > \beta^{-1}$ and the sample is optically opaque (meaning that $\beta l_s \gg 1$), it can be demonstrate that the function $T_m^{T} \cong 1$. In the next Figure, the theoretical acoustic pressure is shown as function

of the relative modulation frequency[1] $f \cdot f_c^{-1}$. This change of variable is more straightforward for theoretical analysis purposes [7, 8], because the equations becomes independent of the material.

Using Eq. (11) and (23), we calculate the spectral power density for the open PA cell configuration, considering that $\omega_c = n\omega$, for some fixed $n \neq 0$,

$$F_m^k = \frac{\sqrt{2\pi}P_{b0}}{1+ir}\sum_{j=-\infty}^{\infty}\frac{d_{m-j}^k \cdot \mathrm{Sinc}(j/2)}{j\omega \cdot \mathrm{Sinh}\sigma_{sj}l_s}T_j^T,$$

$$S_o^k = 2\pi\sum_{m\neq 0}\left|F_m^k\right|^2 \cdot \delta(\omega' - \omega_m). \tag{24}$$

Where $r = m/n$. From here is clear that, even selecting a cut-off frequency for the LPF equal to an arbitrary multiple of the fundamental frequency, the contributions of superior harmonics does not vanishes. From Eq. (24) it can be seen that the factor r contributes with a multiplicative constant in the F_m^k coefficients, and with a relative phase for each harmonic of $\hat{f}_o^k$. However, the average power and the true RMS values of $\hat{f}_o^k$ has no phase shifting, and are only relevant the amplitude of the harmonic contributions. In Figure 6, the calculated spectral power densities are shown, as function of the relative frequency.

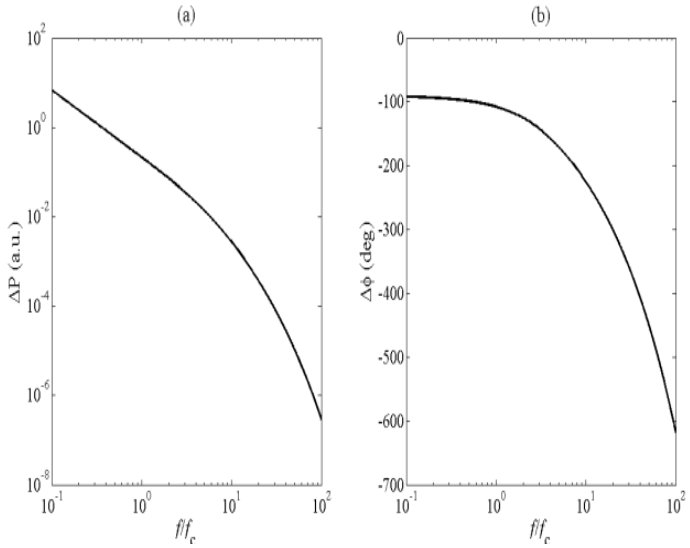

FIGURA 5. Theoretical acoustic pressure, for OPC configuration: (a) Amplitude, and (b) Phase shift.

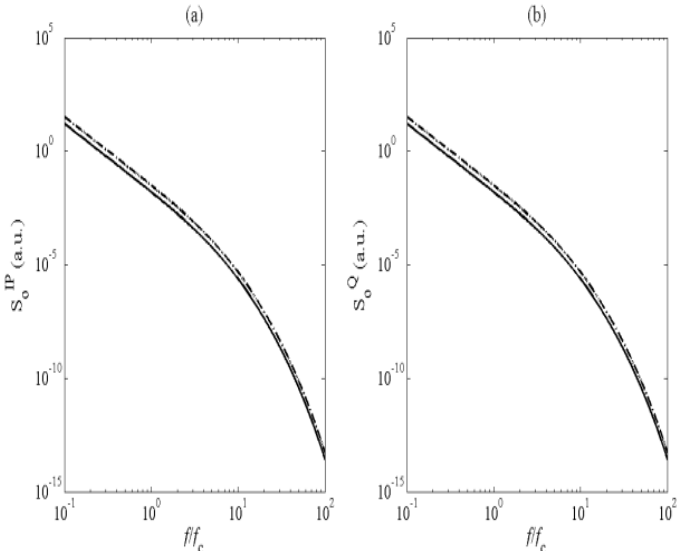

FIGURA 6. Spectral power densities for the OPC configuration: (a) In-phase, and (b) Quadrature components, for values of n = 1(solid line) and n =21 (dashed line).

B. Closed PA cell configuration

In this configuration, the backing medium (b) is a solid, not necessarily a god heat conductor, employed as a support for the sample (and sometimes, closing the air chamber of the PA cell). The medium (g), is the air enclosed in the acoustic chamber. For the diffusion configuration is necessary a transparent window, as shown in Figure 4b.

Based in the Thermal Piston model, the acoustic pressure oscillations are given as follows,

$$\Delta P_g = \frac{\gamma P_{atm}}{l_g T_{amb}}\sum_{m\neq 0}R_{sm}(\omega,0)\int_0^{2\pi\mu_{gm}} e^{-\sigma_{gm}z}dz. \tag{25}$$

And, in this way,

$$\Delta P_g = P_{g0}\sum_{m\neq 0}\frac{\mathrm{Sinc}(m/2)}{m\omega}D_m^T. \tag{26}$$

Being P_{g0} an amplitude factor, independent of the modulation frequency. Because the backing medium is a solid, the expression for D_m^T is more complex than T_m^T,

$$D_m^T = \frac{r_{sm}}{1-r_{sm}^2}\left[1+\frac{U_{bs}}{\mathrm{Sinh}\sigma_{sm}l_s + \eta_{bs}\mathrm{Cosh}\sigma_{sm}l_s}\right],$$

$$U_{bs} = (r_{sm}-\eta_{bs})\cdot e^{-\beta l_s} - r_{sm}\left[\mathrm{Cosh}\sigma_{sm}l_s + \eta_{bs}\mathrm{Sinh}\sigma_{sm}l_s\right]. \tag{27}$$

In Figure 7, we present the theoretical calculations of the acoustic pressure, for the CPC configuration.

[1] The characteristic frequency f_c is defined as the value of the modulation frequency, f, at which the thermal diffusion length equals the sample thickness.

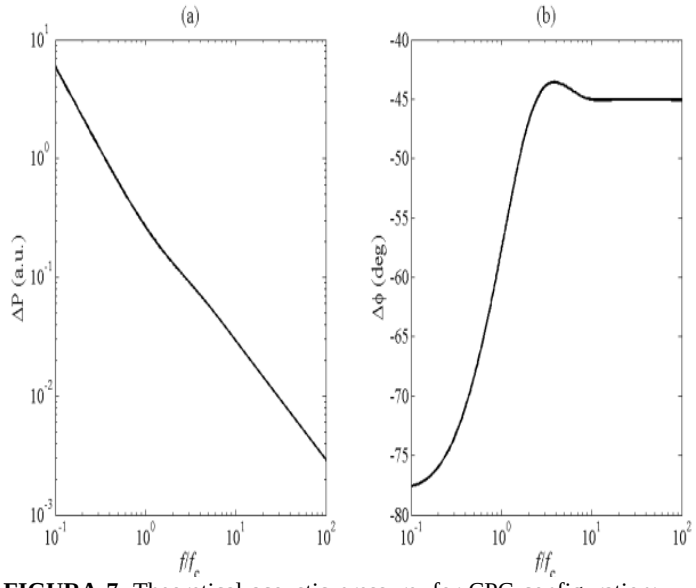

FIGURA 7. Theoretical acoustic pressure, for CPC configuration: (a) Amplitude, and (b) Phase shift.

If occurs that $\mu_{sm} \gg \beta^1$ and the sample is optically opaque (meaning that $\beta l_s \gg 1$), it can be demonstrate that the function D_m^{T} reduces to,

$$D_m^{\mathrm{T}} = \frac{\mathrm{Cosh}\sigma_{sm} l_s + \eta_{bs}\mathrm{Sinh}\sigma_{sm} l_s}{\mathrm{Sinh}\sigma_{sm} l_s + \eta_{bs}\mathrm{Cosh}\sigma_{sm} l_s}. \qquad (28)$$

Similar expressions to Eq. (24) can be founded for the calculation of the spectral power densities in the closed PA cell configuration (see Figure 8). In any case, the spectral power density carries the contribution of the superior harmonics as well the fundamental frequency.

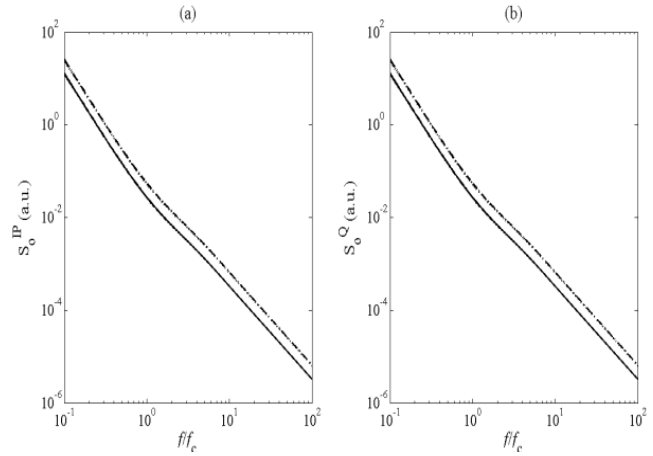

FIGURA 8. Spectral power densities for the CPC configuration: (a) In-phase, and (b) Quadrature components, for values of n = 1(solid line) and n =21 (dashed line).

Note, from Figures 6 and 8, that there is a strong dependence on the modulation frequency of the output power densities (as where expected), and in fact, centering the LPF in a superior harmonic amplifies slightly the output power densities.

VI. CONCLUSIONS

We demonstrate that, for reference signals congruent with the modulation type of the optical excitation signal, the contribution of superior harmonics do not vanishes during the PSD and LPF stages of the amplification and filtering processes of the PA signal. The Eqs. (11, 24) demonstrate that even when the cut-off frequency of the LPF is set to a particular harmonic, the spectral power density carries on the influence of all harmonics, being the most relevant those nearest to the cut-off frequency. This enables us to investigate separately the accumulative contribution of the harmonics in the thermal response, especially when complex thermal relaxation processes are present in the PA signal generation, or in general, in the Photothermal signal generation.

REFERENCES

[1] Marín, E. and Ivanov, R., *LIA in a Nut Shell: How can Trogonometry help to understand Lock-in Amplifier operation?* **3**, 544-546 (2009).
[2] Spears, B. K. and Tufillaro, N. B., A chaotic lock-in amplifier, Am. J. Phys. **76**, 213-217 (2008).
[3] Mandelis, A., *Signal-to-noise ratio in lock-in amplifier synchronous detection: A generalized communications systems approach with application to frequency, time and hybrid (rate window) photothermal measurements,* Rev. Sci. Instrum. **65**, 3310-3323 (1994).
[4] Boashash, B., *Time frequency signal analysis and processing: A comprehensive reference*, (Elsevier Inc., Oxford, 2003).
[5] Arfken, B. G., Weber, H. H. and Harris, F. E., *Mathematical Methods for Physicist*, (Elsevier Inc., Oxford, 2013).
[6] Carslaw, H. S., Jaeger, J. C., *Conduction of heat in solids*, (Clarendon Press, Oxford UK, 2000).
[7] Rojas-Trigos, J. B., Calderón, A, and Marín, E., *Heat diffusion in a homogenous slab with an arbitrary periodical heat source: The case of sinusoidal modulation function*, Lat. Am. J. Phys. Educ. **5**, 712-719 (2011).
[8] Rojas-Trigos, J. B., Calderón, A, and Marín, E., *Heat diffusion in a homogenous slab with an arbitrary periodical heat source: The case of heat source with square wave modulation function*, Lat. Am. J. Phys. Educ. **6**, 59-66 (2012).
[9] Mandelis, A., *Diffusion-wave fields. Mathematical methods and Green functions*, (Springer Verlag, New York, 2001).
[10] Friedman, B., *Principles and techniques of applied Mathematics*, (Dover Publications Inc., New York, 1990).

[11] Rosencwaig, A. and Gersho, A., *Theory of the Photoacoustic effect in solids*, J. Appl. Phys. **47**, 64-69 (1976).
[12] Almond, D. P. and Patel, P. M., *Photothermal science and techniques*, (Chapman & Hall, London, 1996).
[13] Marín, E.: in *Thermal Wave Physics and Related Photothermal Techniques: Basic Principles and Recent Developments*, ed. E. Marín Moares (Transworld Research Network Kerala, India, 2009) Chap. I, p. 1.
[14] Bissieux, C., Pron, H. And Henrry, J. F.: in *Thermal Wave Physics and Related Photothermal Techniques: Basic Principles and Recent Developments*, ed. E. Marín Moares (Transworld Research Network Kerala, India, 2009) Chap. X, p. 253.